The role of three-wave interactions in Faraday wave pattern formation

Laura Pinkney, Alastair Rucklidge, Cédric Beaume

University of Leeds

January 16, 2026

Faraday Wave Experiment

Container of fluid with a free surface is subject to a vertical periodic forcing.
When the amplitude of the forcing exceeds a critical value, the system undergoes an instability (Faraday instability) resulting in patterns formed on the surface.

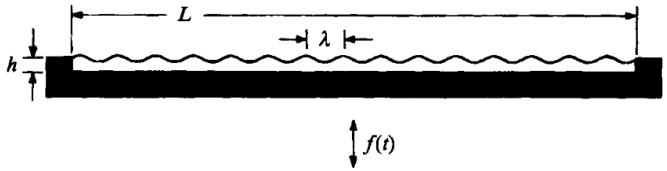

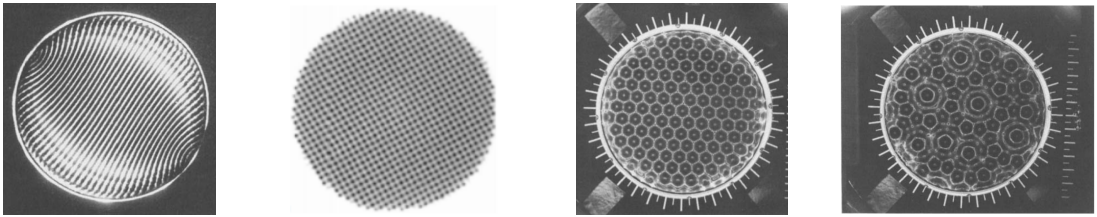

Figure: A container of depth h, and length/width L (both directions) filled with fluid is subject to vertical forcing $f(t)$ and example patterns found experimentally, all from Edwards & Fauve (1994).

Pattern-Forming Systems

We consider pattern-forming systems of the form

$$\frac{\partial u}{\partial t} = \mathcal{L}u + \mathcal{N}(u), \tag{1}$$

where $u = u(x, y, t)$ is the pattern-forming field, $\mathcal{L}$ is a linear operator and $\mathcal{N}(u)$ are nonlinear terms.
Simple example: Swift–Hohenberg equation (SH23)

$$\frac{\partial u}{\partial t} = \mu u - \left(1 + \nabla^2\right)^2 u + Qu^2 - u^3. \tag{2}$$

Example with two-wavelengths: Lifshitz–Petrich equation

$$\frac{\partial u}{\partial t} = \mu u - \left(1 + \nabla^2\right)^2 \left(q^2 + \nabla^2\right)^2 u + Qu^2 - u^3. \tag{3}$$

Two Wavelengths: Linear Theory

We now consider problems where waves with wavenumbers $k = 1$ and $k = q$ $(q < 1)$ both become unstable. They have growth rates μ and ν respectively. We also impose $q < 1/2$.
A mode of the form $e^{\sigma t + i\boldsymbol{k}\cdot\boldsymbol{x}}$ with wavevector $\boldsymbol{k}$ and wavenumber $k = |\boldsymbol{k}|$ grows with growth rate σ:

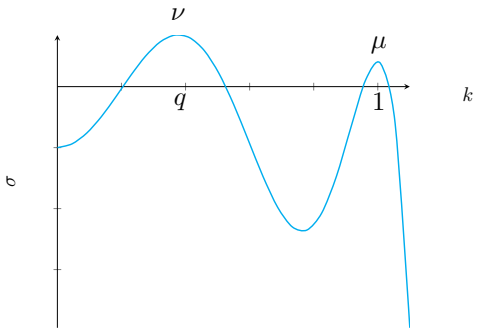

If we increase μ and ν from negative to positive, at $\mu = 0$ $(\nu = 0)$ the trivial state $u = 0$ loses stability, and waves with $k = 1$ $(k = q)$ begin to grow. We write the pattern forming field u as a sum of Fourier modes $e^{i\boldsymbol{k}\cdot\boldsymbol{x}}$ with $|\boldsymbol{k}| = 1$ or $|\boldsymbol{k}| = q$

$$u(x, y, t) = \sum_{|\boldsymbol{k_j}|=1} z_j(t) e^{i\boldsymbol{k_j}\cdot\boldsymbol{x}} + \sum_{|\boldsymbol{q_j}|=q} w_j(t) e^{i\boldsymbol{q_j}\cdot\boldsymbol{x}}. \tag{4}$$

Two Wavelengths, Nonlinear Terms: One Triad

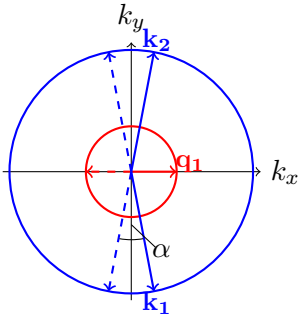

A **resonant triad** is a set of three wavevectors where the sum of two wavevectors gives the third wavevector: $\boldsymbol{q_1} = \boldsymbol{k_1} + \boldsymbol{k_2}$.
Since $q < 1/2$, the only possibility for coupling between both circles comes from two waves on the outer circle and one wave on the inner circle.
Considering just one triad we find the evolution of the amplitudes satisfy

$$\dot{z}_1 = \mu z_1 + Q_{zw}\overline{z}_2 w_1 + z_1\left(A|z_1|^2 + B_\alpha|z_2|^2 + C_{90-\alpha/2}|w_1|^2\right), \tag{5}$$

$$\dot{z}_2 = \mu z_2 + Q_{zw}\overline{z}_1 w_1 + z_2\left(B_\alpha|z_1|^2 + A|z_2|^2 + C_{90-\alpha/2}|w_1|^2\right), \tag{6}$$

$$\dot{w}_1 = \nu w_1 + Q_{zz} z_1 z_2 + w_1\left(E_{90-\alpha/2}|z_1|^2 + E_{90-\alpha/2}|z_2|^2 + D|w_1|^2\right). \tag{7}$$

(Porter & Silber 2004) analysed this system, searching for equilibria and bifurcations as functions of μ and ν. They found the dynamics dependent on the sign of $Q_{zz}Q_{zw}$:

- $Q_{zz}Q_{zw} > 0$: Saddle-node and pitchfork bifurcations. Steady solutions.
- $Q_{zz}Q_{zw} < 0$: Saddle-node, pitchfork and Hopf bifurcations. Steady solutions and time-dependent solutions: periodic and chaotic.

Two Wavelengths: Additional Triads

Triads on both a rhombic lattice (a) and hexagonal lattices (b)–(c)

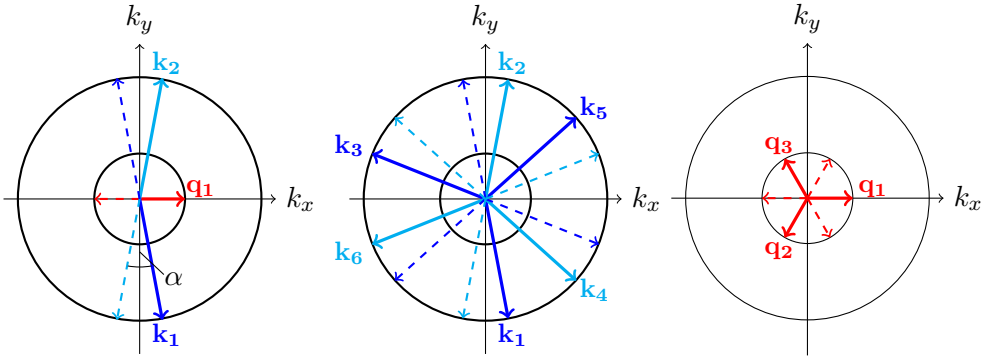

$$\boldsymbol{k_1} + \boldsymbol{k_3} + \boldsymbol{k_5} = 0, \qquad \boldsymbol{k_2} + \boldsymbol{k_4} + \boldsymbol{k_6} = 0, \qquad \boldsymbol{q_1} + \boldsymbol{q_2} + \boldsymbol{q_3} = 0,$$

$$\boldsymbol{q_1} = \boldsymbol{k_1} + \boldsymbol{k_2}, \qquad \boldsymbol{q_2} = \boldsymbol{k_3} + \boldsymbol{k_4}, \qquad \boldsymbol{q_3} = \boldsymbol{k_5} + \boldsymbol{k_6},$$

Two Wavelengths: Amplitude Equations

Using both the rhombic and hexagonal triads, we write a system of 9 complex ODEs:

$$\begin{aligned}\frac{\mathrm{d}z_1}{\mathrm{d}t} =&\mu z_1 + Q_{zw}\overline{z}_2 w_1 + Q_{zhex}\overline{z}_3\overline{z}_5 \\ &+ z_1\left(A|z_1|^2 + B_\alpha|z_2|^2 + B_{60}|z_3|^2 + B_{60-\alpha}|z_4|^2 + B_{60}|z_5|^2\right. \\ &\qquad \left. + B_{60+\alpha}|z_6|^2 + C_{90-\alpha/2}|w_1|^2 + C_{30+\alpha/2}|w_2|^2 + C_{30-\alpha/2}|w_3|^2\right) \\ &+ K_1 z_4 z_6 w_1 + K_2\overline{z}_2\overline{w}_2\overline{w}_3 + K_3 z_4\overline{z}_5\overline{w}_2 + K_4\overline{z}_3 z_6\overline{w}_3, \end{aligned} \tag{8a}$$

$$\begin{aligned}\frac{\mathrm{d}w_1}{\mathrm{d}t} =&\nu w_1 + Q_{zz} z_1 z_2 + Q_{whex}\overline{w}_2\overline{w}_3 \\ &+ w_1\left(E_{90-\alpha/2}|z_1|^2 + E_{90-\alpha/2}|z_2|^2 + E_{30-\alpha/2}|z_3|^2 + E_{30+\alpha/2}|z_4|^2\right. \\ &\qquad \left. + E_{30+\alpha/2}|z_5|^2 + E_{30-\alpha/2}|z_6|^2 + D|w_1|^2 + F_{60}|w_2|^2 + F_{60}|w_3|^2\right) \\ &+ L_{hex} z_2\overline{z}_3\overline{z}_5 + L_{hex} z_1\overline{z}_4\overline{z}_6 + L_1\overline{z}_3\overline{z}_4\overline{w}_3 + L_1\overline{z}_5\overline{z}_6\overline{w}_2. \end{aligned} \tag{8b}$$

The subscripts denote the angle between wavevectors, where α is the angle between $\boldsymbol{k_1}$ and $\boldsymbol{k_2}$.

Amplitude Equations: Simple Equilibria

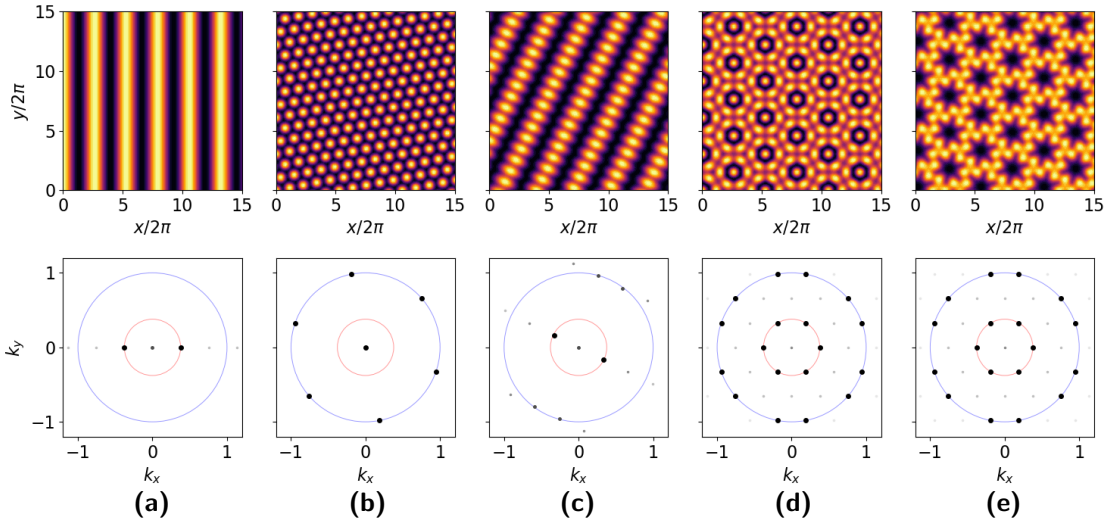

Figure: Simple patterns and their fourier spectrum observed in the amplitude equations (8a)–(8b). (a) stripes, (b) hexagons, (c) rhombs, (d) superhexagons, (e) stars.

Modelling with 3WIs

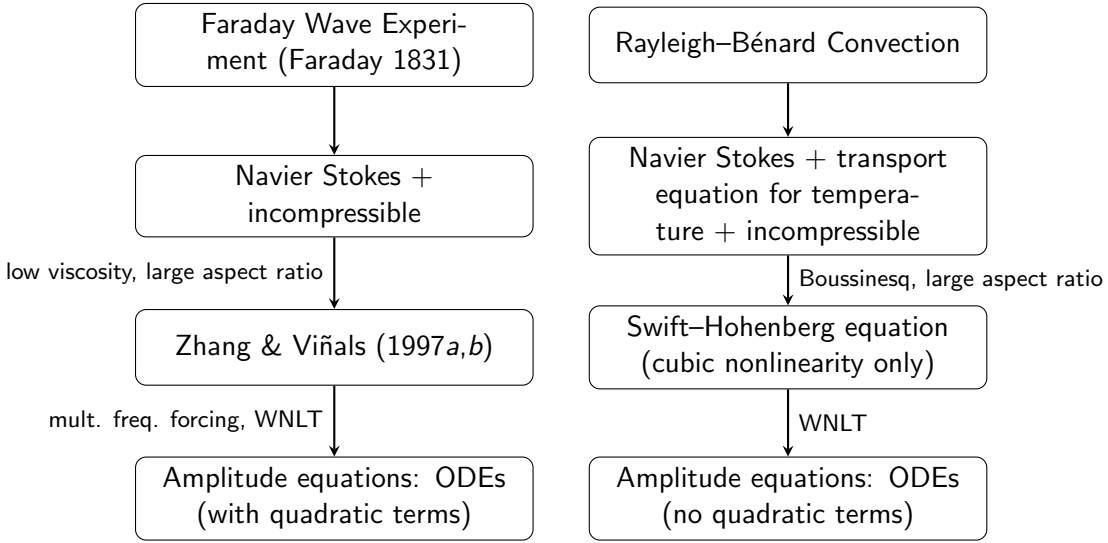

Our Model

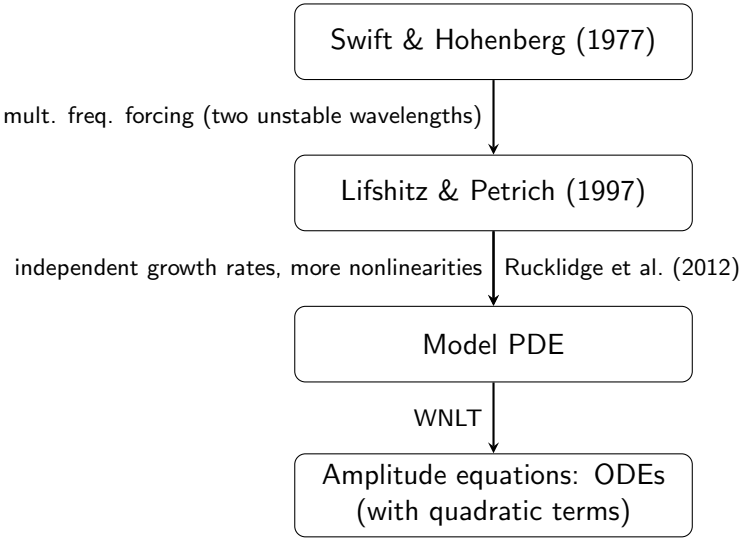
Swift & Hohenberg (1977)
mult. freq. forcing (two unstable wavelengths)
Lifshitz & Petrich (1997)
independent growth rates, more nonlinearities
Rucklidge et al. (2012)
Model PDE
WNLT
Amplitude equations: ODEs
(with quadratic terms)

Model PDE

We now consider a model PDE which is an adaptation of the Lifshitz–Petrich equation

$$\frac{\partial u}{\partial t} = \mathcal{L}(\mu, \nu, q)u + Q_1 u^2 + Q_2 u \nabla^2 u + Q_3 |\boldsymbol{\nabla} u|^2 + C_1 u^3 + C_2 u^2 \nabla^2 u + C_3 u |\boldsymbol{\nabla} u|^2, \tag{9}$$

where $\mathcal{L}$ is the linear operator

$$\mathcal{L} = \frac{-\nabla^2 [A\mu + B\nu]}{q^4 (1 - q^2)^3} + \frac{\sigma_0}{q^4} (1 + \nabla^2)^2 (q^2 + \nabla^2)^2, \tag{10}$$

with

$$A = (\nabla^2 (3 - q^2) - 2q^2 + 4)(q^2 + \nabla^2)^2 q^4, \tag{11}$$

$$B = (\nabla^2 (1 - 3q^2) + 2q^2 - 4q^4)(1 + \nabla^2)^2. \tag{12}$$

When $Q_2 \neq 2Q_3$ or $C_2 \neq C_3$, this breaks the variational structure that the Swift–Hohenberg equation and the Lifshitz–Petrich equation have. Which allows for stable time-dependent solutions.

Numerical Results: $Q_{zz}Q_{zw} < 0$

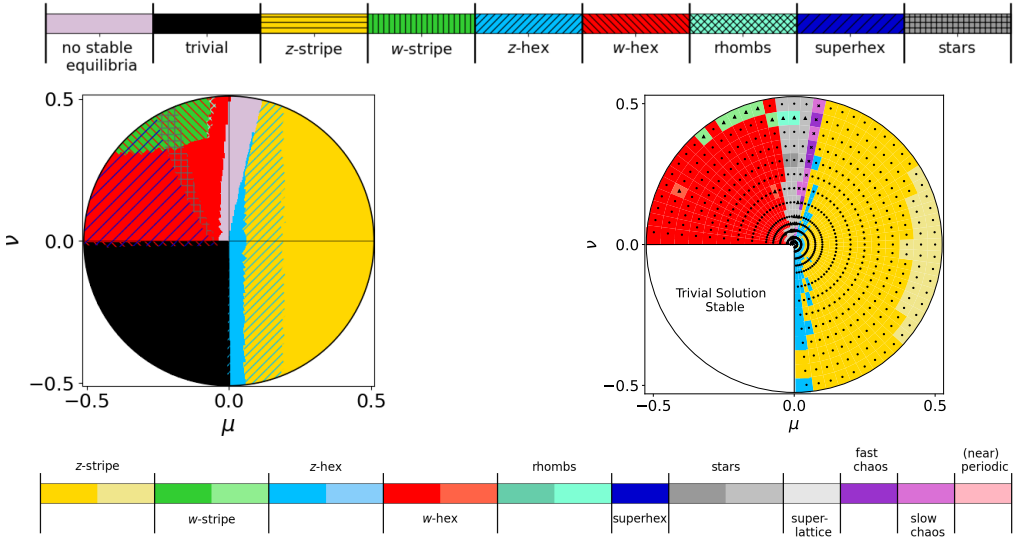

Figure: Comparison of patterns predicted using the amplitude equations with the PDE for $Q_1 = -0.9$, $Q_2 = -2.75$, $Q_3 = -3.5$, $C_1 = -2.75$, $C_2 = -7.75$, $C_3 = -16.5$, $\sigma_0 = -2$, $q = 1/\sqrt{7}$.

Spatiotemporal Chaos

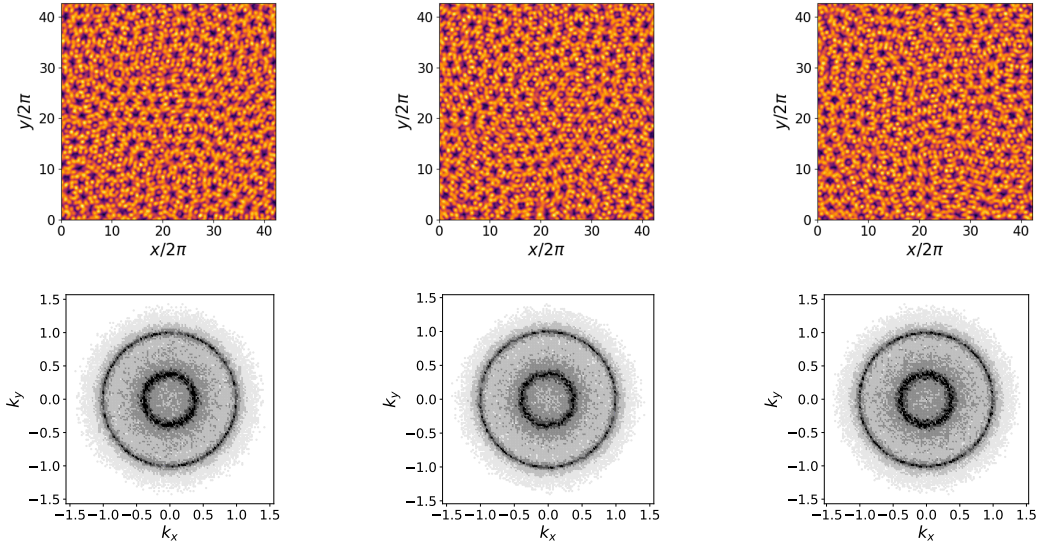

Figure: Frames of a chaotic solution separated by 90 time units for $Q_1 = -1.06$, $Q_2 = -2$, $Q_3 = -0.8$, $C_1 = -1.4$, $C_2 = -5$, $C_3 = -15$, $\sigma_0 = -2$, $q = 1/\sqrt{7}$.

Spatiotemporal Chaos: Faraday Waves

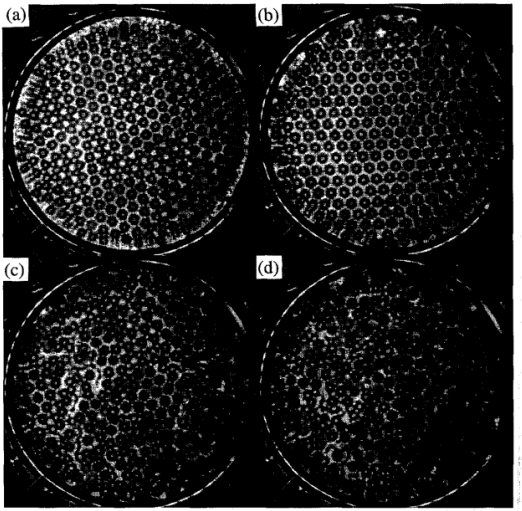

Figure: Kudrolli & Gollub (1996).

Conclusions

- Many types of patterns can arise within the Faraday wave experiment.
- For the case $q < 1/2$, the only possible coupling of three waves between both critical circles comes from two waves on the larger circle and one on the smaller circle.
- 3WI can lead to a variety of patterns, both stationary and time dependent.
- The 3WI amplitude equations are generalised, so can be applied to any pattern forming system with two unstable wavenumbers.
- The amplitude equations can be extremely helpful at predicting dynamics seen PDEs in the weakly nonlinear limit.

References

Edwards, W. S. & Fauve, S. (1994), 'Patterns and quasi-patterns in the Faraday experiment', *J. Fluid. Mech.* **278**, 123–148.

Faraday, M. (1831), 'On the forms and states assumed by fluids in contact with vibrating elastic surfaces', *Phil. Trans. R. Soc. Lond.* **121**, 319–340.

Kudrolli, A. & Gollub, J. (1996), 'Patterns and spatiotemporal chaos in parametrically forced surface waves: a systematic survey at large aspect ratio', *Physica D* **97**(1), 133–154.

Lifshitz, R. & Petrich, D. M. (1997), 'Theoretical model for faraday waves with multiple-frequency forcing', *Phys. Rev. Lett.* **79**, 1261–1264.

Porter, J. & Silber, M. (2004), 'Resonant triad dynamics in weakly damped Faraday waves with two-frequency forcing', *Physica D* **190**(1), 93–114.

Rucklidge, A. M., Silber, M. & Skeldon, A. C. (2012), 'Three-wave interactions and spatiotemporal chaos', *Phys. Rev. Lett.* **108**, 074504.

Swift, J. & Hohenberg, P. C. (1977), 'Hydrodynamic fluctuations at the convective instability', *Phys. Rev. A* **15**, 319–328.

Zhang, W. & Viñals, J. (1997*a*), 'Pattern formation in weakly damped parametric surface waves', *J. Fluid. Mech.* **336**, 301–330.

Zhang, W. & Viñals, J. (1997*b*), 'Pattern formation in weakly damped parametric surface waves driven by two frequency components', *J. Fluid. Mech.* **341**, 225–244.